ORIGINAL RESEARCH

Local and Systemic Delivery of the BimS Gene Nano-Complex for Efficient Oral Squamous Cell Carcinoma Therapy

Pingchuan Ma [1], Jingmei Li [2], Yan Gao[2], Jieping Wu[2], Ke Men [2], Chunjie Li[1], Yi Men[1], Xingmei Duan[3]

[1]State Key Laboratory of Oral Diseases, National Clinical Research Center for Oral Diseases, Department of Head and Neck Oncology, West China Hospital of Stomatology, Sichuan University, Chengdu, Sichuan Province, 610041, People's Republic of China; [2]State Key Laboratory of Biotherapy and Cancer Center, West China Hospital of Sichuan University, Chengdu, Sichuan Province, 610041, People's Republic of China; [3]Department of Pharmacy, Personalized Drug Therapy Key Laboratory of Sichuan Province, Sichuan Academy of Medical Sciences & Sichuan Provincial People's Hospital, School of Medicine, University of Electronic Science and Technology of China, Chengdu, Sichuan Province, 610072, People's Republic of China

Correspondence: Yi Men, State Key Laboratory of Oral Diseases, National Clinical Research Center for Oral Diseases, Department of Head and Neck Oncology, West China Hospital of Stomatology, Sichuan University, Chengdu, 610041, Sichuan Province, People's Republic of China, Email yurimen@163.com; Xingmei Duan, Department of Pharmacy Personalized Drug Therapy Key Laboratory of Sichuan Province, Sichuan Academy of Medical Sciences & Sichuan Provincial People's Hospital, School of Medicine, University of Electronic Science and Technology of China, Chengdu, 610072, People's Republic of China, Email duanxingmei2003@163.com

Purpose: Oral squamous cell carcinoma (OSCC) is the most common type of oral cancer, with more than 300,000 new cases annually. Despite advances in existing treatments, including surgery, radiation, chemotherapy, and immunotherapy, the overall survival and prognosis have remained poor. However, gene therapy based on non-viral vectors provides new ideas for the treatment of OSCC. Here, we aimed to prepare and describe the synthesis, biosafety, and preclinical efficacy of DOTAP-mPEG-PCL (DMP) in OSCC gene therapy.

Methods: We prepared a nano-sized hybrid cationic micelle DMP. DMP micelles were prepared by self-assembling cationic lipid DOTAP and mPEG-PCL polymer. We evaluated the characteristics of this cationic micelle in vitro. Combined with encoding the apoptosis-inducing BimS gene, we established the DMP/phBimS complex and evaluated its anti-tumor effect in vitro. We also established a mouse tongue xenograft model to evaluate the antitumor effect of the DMP/phBimS complex in vivo through local and systemic administration prospectively.

Results: The DMP cationic micelle is spherical in shape, with an average diameter of 28.32 ± 3.56 nm and an average zeta potential of 43.43 ± 0.82 mV. By activation of lipid raft-mediated endocytosis caveolin-mediated endocytosis, DMP could efficiently deliver plasmid into SCC15 cells (efficiency: $52.07\% \pm 1.63\%$), with an ideal biosecurity. When loaded by plasmid encoding the apoptosis-inducing BimS gene, the DMP/phBimS complex exhibited an obvious anti-proliferation effect of SCC15 in vitro through the apoptosis pathway ($33.9\% \pm 2.62\%$ apoptosis rate). By local administration, the DMP/phBimS complex showed ideal anti-tumor properties in the nude mouse tongue xenograft model, with an average tumor inhibition rate of 65.66%. Furthermore, through systematic administration, the DMP/phBimS complex obviously inhibited OSCC growth, with an average inhibition rate of 45.63% (DMP/phBimS) and an appropriate biocompatibility.

Conclusion: The DMP/phBimS complex is an optional effective option for suicide gene therapy for OSCC.

Keywords: gene therapy, Bim, micelle, oral squamous cell carcinoma, non-viral delivery

Introduction

Oral squamous cell carcinoma (OSCC) is one of the most commonly diagnosed neoplasms worldwide, with more than 300,000 new cases annually and accounting for nearly 90% of all oral cancers.[1,2] Currently, the major treatment methods for OSCC include surgery, radiotherapy, chemotherapy, and targeted therapy, either alone or in combination.[3,4] In recent

2925

years, some novel therapies, including gene therapy, have emerged as supplemental optional treatment of OSCC.[5] Treatment based on viral vectors such as Gendicine, a recombinant human serotype-5 adenovirus that contains wild-type tumor suppressor gene p53,[6] was first approved in 2003; however, these viral vectors have not been rapidly developed, and there remains a lack of gene therapy strategies and drugs. Gene therapy based on non-viral vectors have the advantages of safety, high delivery efficiency, and multiple administration,[7] providing new ideas for the development of gene therapy in OSCC.

There are numerous therapeutic cytoreductive strategies in gene therapy design. Among these, suicide gene therapy is another important therapeutic strategy that induces cell apoptosis to achieve anti-tumor effects.[8] Indeed, a previous study indicated that activation of iCaspase-9 in neovascular endothelial cells using biodegradable scaffolds can inhibit the progression of xenografted oral tumors through apoptosis.[9] Moreover, restoring p53 function can also induce apoptosis in cancer cells.[10] Suicide gene therapy has been studied in numerous cancers, and has shown a certified broad spectrum antitumor function.[11] Thus, based on its characteristics, we suspect that suicide gene therapy would also be suitable for OSCC as it directly induces tumor cell apoptosis. The Bcl-2 gene family is another important site for pro-apoptosis suicide gene therapy. Bim (Bcl-2-interacting mediator of cell death) is an important pro-apoptotic member of the Bcl-2 protein family,[12] with three protein isoforms, including BimEL, BimL, and BimS. All three isoforms have pro-apoptotic potential, among which BimS is the most potent apoptosis inducer.[13] Activation of Bim protein leads to the activation of Bax and Bak via the mitochondrial-dependent apoptosis pathway and subsequently induces cell death.[14] Bim is a crucial tumor suppressor gene in lung cancer[15,16] and breast cancer.[17] Thus, introducing exogenous BimS has the potential to be used as a suicide gene target in OSCC suicide gene therapy.

Both viral and non-viral vectors have been used to deliver genes into cells. Compared with viral vectors, non-viral vectors have several advantages, including safety and less-restricted DNA packaging capacity. Non-viral vectors also tend to have lower immunogenicity and improved ability to deliver large genetic payloads with easier synthesizing conditions than viral vectors.[18,19] Currently, with the development of nanotechnology, the progress of nanomaterial-based carriers has increased the number of studies on non-viral vectors. Among them, polymetric nanoparticles are expected to have potential value in gene therapy delivery systems due to their high payload encapsulation efficiency, moderate protection ability, and ability to be customized for utility.[20] Biodegradability and convenient surface modification are other advantages of polymeric nanoparticles.[21,22] A high delivery efficiency and simple synthesis pathway are the basic qualifications for nanovectors in cancer gene therapy. Furthermore, for OSCC, the vector should be sufficiently stable for use in multiple drug delivery patterns, including both local and systemic administration.[23] Simple local administration is difficult for OSCC and has the possibility of drug leaking due to the various tumor sites, while systematic administration could theoretically apply to all related areas. For systemic administration, the vectors should be distributed to target lesion areas, maintaining a moderate duration for therapeutic effect. As a result, the request for gene vectors in OSCC is higher than that in other cancer types. However, only a few studies have attempted to systemically apply non-viral vectors in OSCC, potentially because of the deficiency in nanoparticle preparation technology.[24] Thus, there is demand to develop an appropriate non-viral vector for gene therapy in OSCC, which can be used systemically and have the advantages of safety and efficiency. In our previous studies, we developed a novel non-viral gene delivery system by one-step modification of monomethoxy poly (ethylene glycol)–poly(ε-caprolactone) (mPEG–PCL, MP) micelles with a cationic lipid N-[1-(2,3-dioleoyloxy) propyl]-N, N, N-trimethylammonium methyl-sulfate (DOTAP) to prepare a nano-sized hybrid cationic micelle, DOTAP-mPEG-PCL (DMP).[25,26] Prepared DMP micelles have been demonstrated to possess effective gene delivery ability with an ideal safety profile in anti-tumor studies.[27] Several studies have examined systemic administration of DMP, indicating that it can be used in a variety of tumors and nucleic acid forms with suitable protection ability.[26] Its distribution in the circulatory system and its biosecurity or biodegradation have been verified in other cancers but have not yet been explored in OSCC. We suspect that DMP is an eligible nanoparticle non-viral vector for use in a gene therapy delivery system in OSCC.

In this study, we focused on DMP micelles and plasmids containing the BimS gene to prepare the DMP/phBimS complex. We hypothesize that the DMP vector can be used to efficiently deliver plasmid BimS through multiple administration pathways to tongue squamous cell carcinoma to play a therapeutic role. The properties and plasmid DNA delivery capacity of DMP nanoparticles were characterized. The therapeutic potential anti-cancer effect of the

DMP/phBimS complex was evaluated in vitro and in a tongue cancer animal model. The in vivo distribution, degradation, and excretion were also investigated.

Materials and Methods

Chemicals and Plasmids

The method of synthesis of DOTAP-mPEG-PCL (DMP) micelles has been described previously.[25] Polyethyleneimine (PEI25K) and 3-(4,5-dimethylthiazol-2-yl)-2,5-diphenyltetrazolium bromide (MTT) were purchased from Sigma-Aldrich Inc® (USA); GoldView II Nuclear Staining Dyes were purchased from Solarbio®; pre-stained protein ladders and DNA ladders were obtained from Fermentas (Thermo Fisher Scientific®, USA); and the plasmid encoding hBimS (phBimS) was constructed using a pVAX1 plasmid vector between the BamH I and Xba I sites (Invitrogen Corporation®, USA), which is an expression vector encoding kanamycin resistance. The PVAX1 plasmid without hBimS-cDNA was used as an empty vector. The pVAX- hBimS plasmid DNA (phBimS) was propagated in *Escherichia coli*. Colonies of *E. coli* containing phBimS or pVAX were cultured in Luria-Bertani broth containing kanamycin (100 μg/mL). The large-scale plasmid DNA used in this study was purified using an EndoFree Plasmid Giga kit (Qiagen®, USA) in accordance with the manufacturer's instructions. The purified DNA was then dissolved in sterile endotoxin-free water and frozen at –20°C before use. The recombinant phBimS was confirmed by DNA sequencing.

Cell Lines

Human tongue squamous carcinoma cells are highly aggressive and migratory, and are commonly used to represent a tumor-progression model of OSCC.[28] SCC15 (a human tongue squamous cell carcinoma cell line) and 293T (a human embryonic kidney cell line) were purchased from the American Tissue Type Collection (ATTC). The cell lines were cultured in Dulbecco's modified Eagle's medium (DMEM) containing 10% fetal bovine serum (FBS; Cell-Box, Aoke Biotechnology, Chengdu), with 100 U/mL penicillin and 100 μg/mL streptomycin in a 5% CO_2 humidified air atmosphere at 37°C.

Animals

Six to eight-week-old female BALB/c nude mice were purchased from Beijing HFK Bioscience Co., Ltd® (Beijing, China) and maintained under specific pathogen-free (SPF) conditions. The animal experiments were conducted under the approval of the Institutional Animal Care and Treatment Committee of Sichuan University and the processes were performed according to the Guidelines and Standard Operating Procedure (SOP) for Laboratory Animals of Sichuan University.

Gene Transfection in vitro

The transfection efficiency of the DMP/plasmid complex was measured using a flow cytometer. SCC15 or 293T cells were seeded into a 24-well plate at 3×10^4 cells per well with 500 μL of DMEM medium containing 10% FBS. Twenty-four hours later, the DMEM medium in wells (containing 10% FBS) was changed to serum-free DMEM medium. We mixed 1 μg of plasmid encoding enhanced GFP (EGFP) with PEI25K (1:1, w/w) and DMP (20:1, w/w) prospectively in 100 μL of DMEM medium without serum. The concentration of DMP in this transfection system was 0.2 μg/μL. We added the complexes to the cells 15 min after mixing. Four hours later, serum-free DMEM medium was transformed to DMEM medium (containing 10% FBS) and incubated at 37°C. PEI25K/EGFP (1:1, w/w) was used as the transfection control. After 24 h, the cells were photographed by a fluorescence microscope to obtain images. The transfection efficiency was detected by flow cytometry (NovoCyte Flow Cytometer, ACEA Biosciences Inc®, USA). Plasmid transfection in the subsequent experiment was performed using the same protocol as the methods outlined above.

Preparation and Characterization of Micelles

We prepared DMP micelles by self-assembly of DOTAP with mPEG-PCL. Briefly, 5 mg N-[1-(2,3-dioleoyloxy) propyl]-N, N, N-trimethylammonium methyl-sulfate (cationic lipid DOTAP, Avanti) and 45 mg mPEG-PCL polymer (Ruixibio®, China)

(1:9, w/w) were dissolved using methylene dichloride (KeLong Chemicals®, China) followed by 1 h of rotary evaporation with heat to obtain a lipid film. The lipid film was then rehydrated in 5 mL double-distilled water at a final concentration of 10 mg mL^{-1} at a temperature of 55°C. The prepared DMP was stored at 4°C before use.

The size distribution and zeta potential of the DMP cationic micelles were tested by dynamic light scattering (Malvern®, UK). The measurement process was performed at 25°C after equilibration. A transmission electron microscope (TEM) (FEI Tecnai G2 F20 S-TWIN, USA) was used to observe the morphology of DMP. The DMP/plasmid was prepared by incubation of DMP and plasmid at a ratio of 20:1 (w:w) at room temperature.

Cellular Uptake Mechanism of the DMP/Plasmid Complex

To investigate the main endocytosis mechanisms of the DMP/plasmid, we treated SCC15 cells with amiloride (2 mM), genistein (420 μM), chlorpromazin (2.5 μg/mL), methyl-β-cyclodextrin (8 mM), and NaN$_3$ (14 mM)/ 2-Deoxy-D-Glucose (140 mM) for 30 min before transfection by the DMP delivering EGFP plasmid as mentioned above. Then, 24 h after transfection, we measured the transfection efficiency by flow cytometry. We also examined the cells under a fluorescence microscope and photographed them after staining with Hoechst and Dil, which dye the cell membrane (Solarbio®).

Anticancer Activity of DMP/phBimS Complexes on SCC15 Cells in vitro

To verify the apoptosis effect of the DMP/phBimS complex, we conducted the transfection process in SCC15 cells. Briefly, SCC15 cells were seeded into a 24-well plate at 1×10^4 per well. Next, DMP, DMP/pVAX (2 μg plasmid per well), and DMP/phBimS (2 μg plasmid per well) with a 20:1 weight ratio were transfected into wells (4 wells per group) according to the protocol mentioned above. The concentration of DMP was 0.4 μg/μL in transfection system. The plate was incubated at 37°C, before conducting the same transfection process 24 h and 48 h after cell seeding. Next, 48 h after the second transfection, the cells were harvested and stained with Annexin V-fluorescein isothiocyanate (FITC) and propidium iodide (Genechem®) and analyzed by flow cytometry (NovoCyte Flow Cytometer, ACEA Biosciences Inc®, USA). The same process was conducted on 293T cells with 4×10^4 cells per well seeded in a 24-well plate.

In vivo Fluorescence Imaging

We used an in vivo imaging system (Caliper Life Sciences Inc.®) to detect the distribution tendency of DMP in nude mice. SCC15 cells were maintained in DMEM containing 10% FBS at 37°C in 5% CO$_2$. Nude mice were injected with cultured SCC15 cells into the tip of the tongue (5×10^6 cells suspended in 60 μL of serum-free DMEM) after anesthesia by sodium pentobarbital (50 mg/kg body weight) to establish the mouse tongue xenograft model. Two weeks after injection, mice were intravenously injected with DMP conjugated with Cy5.5 dye (1 μg per mouse). After injection at 5, 15, 30, 60, 120, and 240 min, mice were euthanized and their tongues were harvested. The hearts, livers, spleens, lungs, and kidneys of the mice euthanized 240 min after injection were also harvested. The organs were placed into the imaging chamber platform, and the images of each mouse were recorded by IVIS Spectrum (PerkinElmer®). Meanwhile, the fluorescence intensities of the region of interests (ROI) were analyzed by Living Image Software 3.2.

In vivo Tumor Inhibition Assay

We also evaluated the therapeutic effect of DMP/phBimS in the mouse tongue xenograft model using 6–8-week-old female nude mice. SCC15 cells were injected into the tip of the mouse tongues (5×10^6 cells suspended in 60 μL of serum-free DMEM) after anesthesia with sodium pentobarbital (50 mg/kg body weight) to establish the mouse tongue xenograft model. We used this model to evaluate the therapeutic effect of two drug delivery methods. The mice were randomly divided into four groups after injection of SCC15 cells: Normal saline (NS), DMP (160 μg), DMP/pVAX (8 μg plasmid), and DMP/phBimS (8 μg plasmid) were injected in the tongues of each group 24 h after the injection of SCC15 cells, with a weight ratio of DMP:plasmid of 20:1. The first six treatments were conducted every 24 h and the later treatments were conducted every 48 h. The body weight and tumor size were also measured during the treatment process. The tumor volume was calculated according to the following equation: V = (a × b^2) × 0.5 (V: volume, a: width, and b:

thickness) using a digital caliper. The mice were euthanized on day 24, and their tongues and internal organs (heart, liver, spleen, lungs, and kidneys) were harvested.

The other mice were intravenously injected with normal saline (NS), DMP (200 μg), DMP/pVAX (10 μg plasmid), or DMP/phBimS (10 μg plasmid) 48 h after inoculation of SCC15 cells in tongue with a weight ratio of DMP:plasmid of 20:1. The intravenous injection of drug was conducted every 48 h. The body weight and tumor size of the mice were measured during the treatment process as outline above. On day 18, all mice were euthanized and their tongues and internal organs (heart, liver, spleen, lungs, and kidneys) were harvested. All of the tissues and organs were stored in 4% paraformaldehyde for further use.

Immunohistochemistry Analysis

We examined the specific protein expression in tumors through a series of immunological antibody reactions. Tongue tissues and other organs were fixed with 4% paraformaldehyde. After dehydration and transparency treatment, the appropriate tissue parts were chosen for embedding in paraffin wax. The tissues were sectioned into 3–4-μm thick sections, which were hydrated sections and stained with hematoxylin-eosin (H&E).

We used the terminal deoxynucleotidyl transferase dUTP nick-end labeling (TUNEL) kit (Promega®) to detect apoptosis in tongue tumors. In addition, the paraffin sections were blocked with 3% hydrogen peroxide and stained with Bim (1:200; Cell Signaling Technology®, C34C5), caspase-9 (1:300; Abcam, ab202068), CD8 (1:250; Abcam®, ab203035), and caspase-3 (1:1000; Abcam®, ab84787) primary antibodies overnight at 4°C to identify the exact mechanisms of Bim in tumors. Sections were incubated with anti-CD31 (1:50; Abcam®, ab28364) to evaluate vascular endothelial growth factor expression in tumor vessels. After incubating overnight at 4°C, the tissue sections were treated with a horseradish peroxidase-conjugated secondary antibody and photographed using a fluorescence microscope (Olympus®, Japan).

Blood Tests

Blood tests are a standard method for evaluating the safety of biomaterials in vivo. Female 6-week BALB/c nude mice were divided into three groups and then intravenously injected with NS or DMP/phBimS (20:1, w:w). After 24 h, the blood was collected and the blood index analyzed, including the mean corpuscular volume (MCV), mean platelet volume (MPV), hemoglobin (HGB), mean corpuscular hemoglobin concentration (MCHC), red blood cells (RBCs), platelet distribution width (PDW), and mean corpuscular hemoglobin (MCH). Several liver and kidney function indices were also detected, including alanine aminotransferase (ALT), aspartate aminotransferase (AST), γ-glutamyl transpeptidase (γ-GT), urea (UREA), creatinine (CREA), and uric acid (UA).

Statistical Analysis

All quantitative data are presented as the mean ± standard deviation (SD), and P-values < 0.05 were considered statistically significant. Data were analyzed by two-tailed t-test or one-way analysis of variance (ANOVA) using GraphPad Prism 8.0 software (GraphPad Software®, San Diego, CA, USA). The specific protocols of plasmid gel retardation assay, cytotoxicity assay, quantitative real-time polymerase chain reaction (QPCR), clonogenic assay, anti-proliferation assay, and Western blot analysis are listed in the supplementary information.

Results

Preparation and Characterization of DMP

We first prepared DMP cationic micelles based on the cationic lipid DOTAP and the di-block polymer MPEG-PCL (Figure 1A). DMP nanoparticles were prepared by the self-assembly of these two elements. The average diameter of the prepared DMP was 28.32 ± 3.56 nm, with an average zeta potential of 43.43 ± 0.82 mV (Figure 1B and C). We then evaluated the binding ability of DMP cationic micelles with DNA plasmid using a gel-retarding assay. As the dosage of DMP was increased, the plasmid was gradually bound by the DMP nanoparticles, and the DNA band was weakened. When the weight ratio of DMP:DNA plasmid was 20:1, the DNA plasmid band in the agarose gel was barely visible,
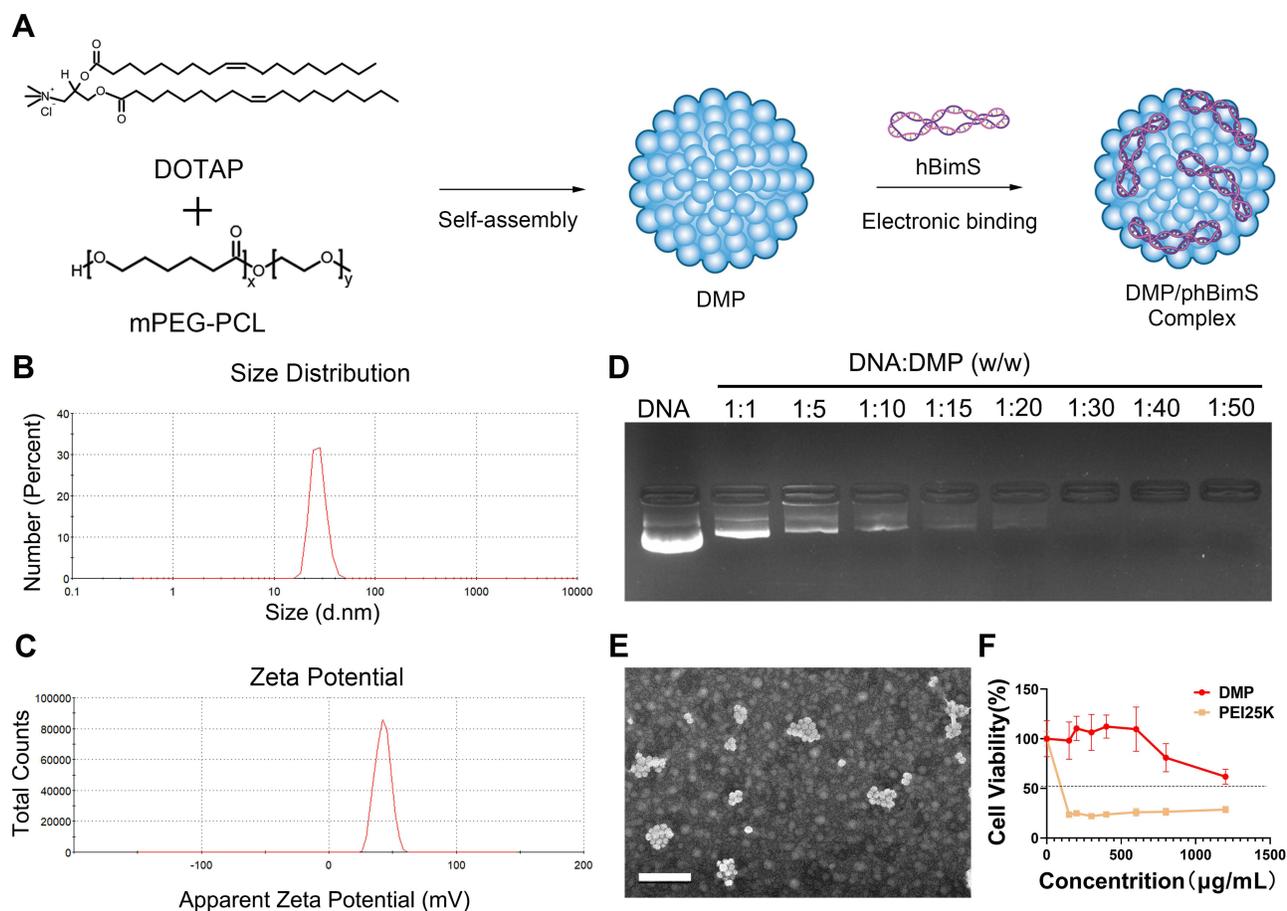
Figure 1 Preparation and characterization of the DMP/phBimS complex. (**A**) Preparation process of the DMP/phBimS complex. (**B**) Size of the DMP cationic micelle. (**C**) Zeta potential distribution of the DMP cationic micelle. (**D**) Gel retarding assay of the DMP/phBimS complex. (**E**) Transmission electron microscopy (TEM) photomicrographs of DMP (scale bar: 200 nm). (**F**) Cell viability assay of the action of DMP and PEI25K on 293T cells.

indicating that this ratio was suitable and sufficient for further evaluation (Figure 1D). Based on the results of gel regarding assay, the plasmid loading rate was determined by quantitative analysis. When the weight ratio of DMP: phBimS was 20:1, the calculated loading rate was 0.89%.

We also observed the morphology of the prepared DMP through TEM. The DMP micelles were monodispersed in a spherical shape (Figure 1E) and the average diameter of DMP under TEM was approximately 50 nm, which was coincident with our results. And the toxicity of DMP micelles toward 293T cells was evaluated using MTT assay. As shown in our results, the IC_{50} of DMP was > 1200 μg/mL, while the IC_{50} of PEI25K was < 150 μg/mL (Figure 1F), indicating that DMP has increased safety compared with PEI25K.

In vitro Gene Transfection Study

We next evaluated the plastic gene delivery capacity of DMP micelles using both human normal 293T cells and human tongue squamous carcinoma SCC15 cells in vitro. The results showed that both the 293T cells and the SCC15 cells could be successfully transfected by the DMP/pEGFP complex (1 μg plasmid per well). The transfection efficiency in 293T cells was 80.11% ± 3.07% and 75.86% ± 3.79% for DMP and PEI25K, respectively, and for SCC15, the transfection efficiency was 52.07% ± 1.63% and 65.81% ± 2.71% for DMP and PEI25K, respectively (Figure 2). The results indicated that the plastic transfection ability of DMP was accessible and effective for both SCC15 and 293T cells for further use. We also observed more obvious cell damage, swelling, and shrinking in the PEI25K group compared with the DMP group, further demonstrating the cytotoxicity of PEI25K. This was also verified in our following exploration.
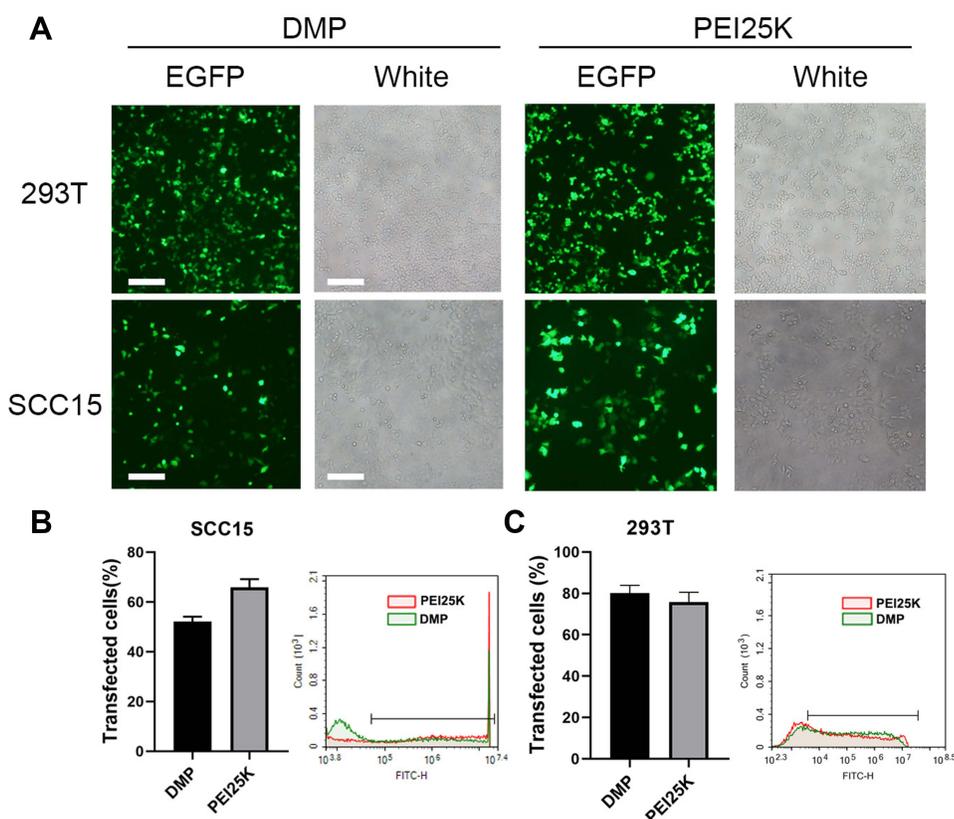
Figure 2 In vitro plasmid transfection study of the DMP/phBimS complex. (**A**) Fluorescent images of transfected SCC15 and 293T cells (scale bars: 200 μm). (**B**) Transfection efficiency on SCC15 cells analyzed by flow cytometry. (**C**) Transfection efficiency on 293T cells analyzed by flow cytometry.

Internalization Mechanism Study of the DMP/Plasmid Complex

We further evaluated the uptake mechanism of the DMP/plasmid complex in SCC15 cells. There are four general internalization mechanisms of nanosized cargos, including lipid raft, caveolin-mediated, clathrin-mediated, and micropinocytosis. Before transfection by DMP micelles with plasmid encoding GFP, we treated SCC15 cells with different inhibitors (methyl-β-cyclodextrin for lipid raft-mediated endocytosis, amiloride for micropinocytosis, NaN_3/2-Deoxy-D-Glucose for the oxidative phosphorylation pathway,[29] genistein for caveolin-mediated endocytosis, and chlorpromazin for clathrin-mediated endocytosis). Twenty-four hours after transfection, we observed the fluorescence and tested the transfection efficiency by flow cytometry. After treatment with methyl-β-cyclodextrin and genistein, the efficiency and fluorescence intensity decreased significantly compared with the untreated cells (Figure 3A). Regarding the flow cytometry results, the transfection efficiency of methyl-β-cyclodextrin and genistein groups was only 20.24% (methyl-β-cyclodextrin) and 16.91% (genistein) (Figure 3B). Meanwhile, cells treated with wortmannin and NaN_3/2-Deoxy-D-Glucose also showed decreased efficiency, although the phenomenon was not prominent according to the microscope images. These findings suggest that lipid raft-mediated and caveolin-mediated endocytosis are the main uptake mechanisms of the DMP/plasmid complex in SCC15 cells.

DMP/hBimS Complex Inhibits SCC15 Cell Proliferation in vitro

As the apoptosis-induction effect was based on successful transfection of the DMP/hBimS complex. We first verified if the pVAX-hBimS plasmid was delivered into SCC15 cells. We used qRT-PCR to evaluate the intracellular mRNA transcription level of the hBimS gene after transfection. Compared to the other three groups, significantly higher hBimS mRNA levels were detected in the DMP/phBimS complex treated group 24 h after transfection (P < 0.05) (Figure 4A). We also tested the BimS protein expression level through Western blot, and found that the protein level was significant
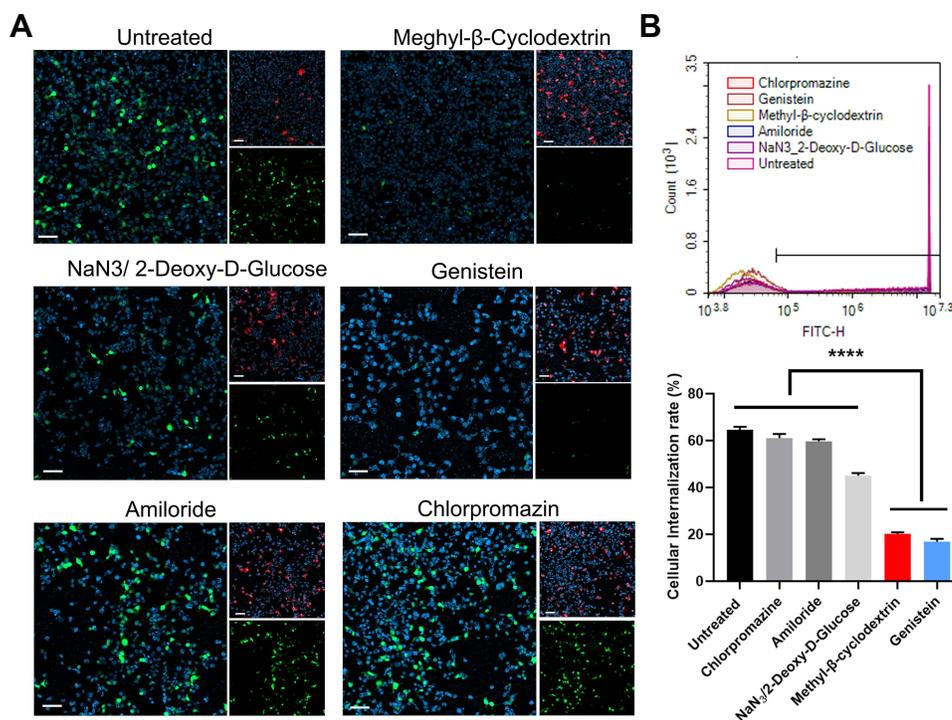
Figure 3 Uptake mechanism study of the DMP/plasmid complex in SCC15 cells. (**A**) Fluorescent images of internalization of the DMP-039/plasmid complex after pre-treatment by different pathway inhibitors. EGFP plasmid in green (EGFP), cell nuclei in blue (Hoechst), and plasma membranes in red (Dil) (scale bar: 100 μm). (**B**) Cell uptake efficiencies analyzed by flow cytometry (****$P < 0.0001$).

higher in the DMP/phBimS group (Figure 4B). This phenomenon suggested high delivery and expression efficiency of DMP/hBimS complex.

Furthermore, as the anti-proliferation effect of the DMP/phBimS complex may be due to the apoptosis induction of BimS protein, we evaluated this process by MTT assay. Our results indicated that compared to the untreated and DMP groups, when SCC15 cells were transfected with the DMP/phBimS complex the cell viability was significantly decreased (Figure 4C and D). In the DMP/phBimS group, only an average of 57.9% cells survived, while in the DMP group, the average survival rate was 84.3% ($P < 0.05$), demonstrating the anti-proliferation effect of the DMP/ phBimS complex.

We also used a clonogenic assay to evaluate the ability of the DMP/phBimS complex to induce cell growth inhibition. As shown in Figure 4E and F, there were fewer SCC15 cell clones in the DMP/phBimS group compared to the other three groups. The average number of cell clones of the DMP/phBimS group was 48.7 ± 5.5, while that of the untreated group, DMP group, and DMP/pVAX group was 278 ± 8.6 ($P < 0.0001$), 268 ± 9.4 ($P < 0.0001$), and 251.3 ± 26.1 ($P < 0.001$), respectively. The results also indicated the anti-proliferation effect of the DMP/phBimS complex, which was consistent with the result of the MTT assay. The hBimS plasmid can be successfully transfected into SCC15 cells by DMP micelles and expressed to inhibit cell growth in vitro.

Bim is an important member of the pro-apoptotic BH3-only Bcl-2 family of proteins that has been reported to induce cell apoptosis. BimS is one of the three predominant splicing variants of Bim. Thus, we further studied whether the cell growth inhibition was the result of apoptosis induction. According to our results, the DMP/phBimS complex caused obvious cell apoptosis (Figure 4G). The average apoptotic cell rate for the DMP/phBimS complex group was 33.9% ± 2.62% via Annexin V/PI staining, while that of the DMP/pVAX and DMP groups were 13.74% ± 3.76% and 3.77% ± 1.2%, respectively ($P < 0.01$). The same process was applied on human embryonic kidney cell line 293T as well.

No obvious apoptosis was observed in 293T cells (Figure S1). These results suggest that the DMP/phBimS complex can efficiently suppress SCC15 cell growth by inducing apoptosis but this induction effect did not occur on 293T cell.
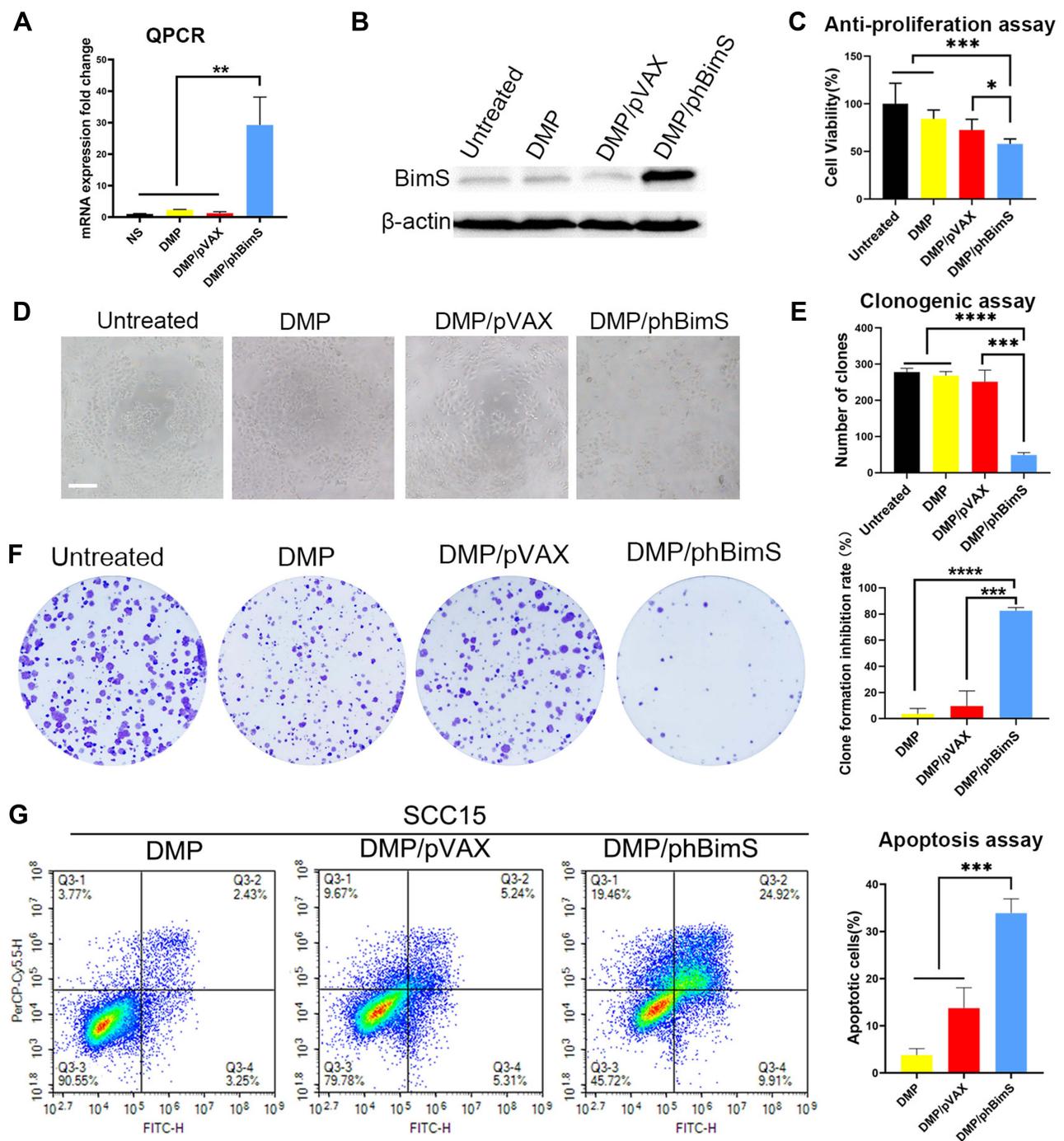
Figure 4 In vitro anti-cancer effect of the DMP/phBimS complex. (**A**) Intracellular level of BimS mRNA in SCC15 cells after transfection (**P < 0.01). (**B**) Level of BimS protein in each treatment group. (**C**) Cell viabilities that measured through the MTT assay (*P < 0.05, ***P < 0.001). (**D**) Image of SCC15 cells after treatment with the DMP/phBimS complex via MTT assay (scale bar: 200 μm). (**E**) Calculate of clone numbers detected by clonogenic assay (***P < 0.001, ****P < 0.0001). (**F**) Detection of the anti-proliferation effect of the DMP/phBimS complex by clonogenic assay; the inhibition rates were calculated based on the clone numbers of each group (***P < 0.001, ****P < 0.0001). (**G**) The DMP/phBimS complex induced apoptosis efficiently in SCC15 cells after transfection, as measured by flow cytometry (***P < 0.001).

DMP/phBimS Complex Suppresses the SCC15 Mouse Tongue Xenograft Model Through Local Administration

We next verified the treatment effect of the DMP/phBimS complex on the nude mouse SCC15 tongue xenograft model. The overall experiment design is shown in Figure 5A. The therapeutic effect of the DMP/phBimS complex was first
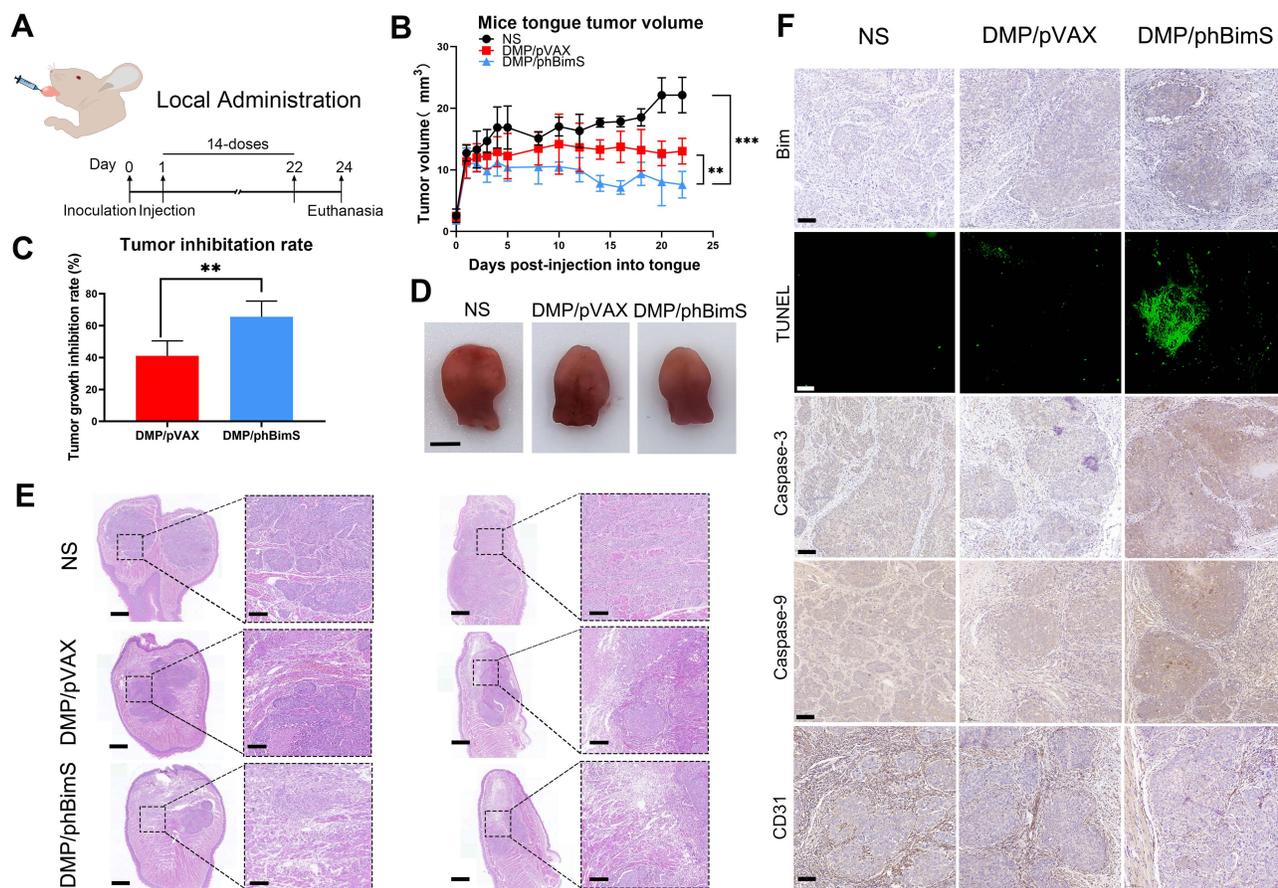
Figure 5 DMP/phBimS complex inhibited tongue squamous cell tumor growth in vivo through local administration. (**A**) Schematic view of the experimental design. (**B**) Trend of the change of the mice tongue volume in each group (**P < 0.01, ***P < 0.001). (**C**) Tumor growth inhibition rate in each group (**P < 0.01). (**D**) Representative isolated tongue from each group (scale bar: 2.5 mm). (**E**) H&E analysis of the tongue tissue of each group (scale bar: 750 μm for entire image; scale bar: 150 μm for partial image.). (**F**) Immunohistochemical evaluation of tumor tissues from each group (scale bar: 100 μm).

evaluated by local administration. Three treatments were directly injected into the tongues of mice in each group, as follows: NS, DMP/pVAX (8 μg) complex, and DMP/phBimS (8 μg) complex. The weight ratio of DMP:plasmid was 20:1. During the observation, the tumor volume in the DMP/phBimS group was smaller than that in the other two groups (Figure 5B), exhibiting an obvious anti-cancer effect. The trend of tumor volume was recorded during this process, and the same trend was verified by the measure of tumor volume. In the initial stage of the observation, the swelling gradually increased in the tongues of mice in all three groups as the tumors developed. However, during the later periods, mice treated with the DMP/phBimS complex exhibited a reduced tumor volume trend. The mice of the DMP/pVAX group maintained a stable tumor volume, while those of the NS group showed a continuous increase in tumor volume. The inhibition rate also showed the therapeutic effect of the DMP/phBimS complex, with an average rate of 65.66% (Figure 5C), which was statistically higher than that of the DMP/pVAX group. A representative tongue image demonstrates the smaller volume in the DMP/phBimS group after euthanasia (Figure 5D).

We also recorded the weight of the mice during the observation. Though the statistical results showed no significant difference between the three groups, in the last stage of observation, the mice of the NS group demonstrated an obvious weight decrease compared with those of the DMP/phBimS group (Figure S2A). H&E staining of the tongue also showed the volume difference between those three groups (Figure 5E). Tongues of the DMP/phBimS group revealed a smaller tumor size in sections, irrespective of whether the sections were lengthwise or across. These results confirm the anti-tumor effect of the DMP/phBimS complex in the tongue xenograft model at an early stage.

We then studied the therapeutic mechanism of the DMP/phBimS complex by immunohistochemistry (IHC). Comparing the NS and DMP/pVAX groups, more positive Bim protein signals were observed in the DMP/phBimS

complex group (Figure 5F), which indicated that Bim can be expressed in tumor tissue following DMP/phBimS delivery. As the Bim gene can induce cancer cell apoptosis, we evaluated the expression of apoptosis-related proteins in the tumor tissues. According to the TUNEL assay, we observed an increase in positive cells in DMP/phBimS complex-treated mice compared with the other two groups (Figure 5F). Additionally, there were strong positive signals in caspase-9- and caspase-3-stained tumor sections in the DMP/phBimS complex group, also suggesting obvious apoptosis induction after the delivery of the DMP/phBimS system. Meanwhile, CD31 staining, demonstrating microvessel formation in tumor tissue, was inhibited by DMP/phBimS complex treatment, suggesting anti-angiogenetic effects.

The biocompatibility of DMP nanoparticles was confirmed as no obvious abnormal or pathology changes were observed in the other main organs of mice by H&E staining (Figure S3A). These results indicate that the DMP/phBimS complex delivery system could effectively deliver phBimS into the mouse SCC15 tongue xenograft model through local administration, as well as induce significant rates of apoptosis in tumor tissue leading to inhibition of SCC15 in early-stage abdominal tumor growth.

DMP/phBimS Complex Suppresses the SCC15 Mouse Tongue Xenograft Model Through Systemic Administration

Based on the mouse SCC15 tongue xenograft model, we decided to explore whether a different method of drug administration could influence the treatment result. Thus, we evaluated the therapeutic potential of systemic administration on the mouse SCC15 tongue xenograft model. For intravenous administration, there is greater concern about the distribution and safety issues of gene delivery systems than simple local administration. Thus, we first evaluated the in vivo distribution of the DMP micelle nanoparticles. To this end, we injected DMP conjugated with Cy5.5 dye (1 μg per mouse) through the tail vein 2 weeks after SCC15 was injected into the tongue, and then detected the in vivo fluorescence images of the tongue. As shown in Figure 6A, from the 5 min timepoint, the excised tongue tissue with a longer time after intravenous injection showed a higher fluorescence intensity. At the 4 h timepoint, the tongue showed the highest fluorescence intensity, which indicated the DMP could still gather in the tongue area 4 h after intravenous injection. Indeed, fluorescence could be detected only 5 min after injection, indicating that through systematic administration, DMP could effectively distribute in the tongue area for at least 4 h. Furthermore, at the 4 h timepoint after injection, we detected the fluorescence intensity in the main organs of mice (Figure 6B). In addition to the tongue area, fluorescence was detected in the lung (15.5%), kidney (13.0%), spleen (5.3%), liver (52.3%), and heart (5.4%). The highest fluorescence was detected in the liver, indicating that most metabolic processes of DMP occurred in the liver, while considerable fluorescence was still detected in the tongue area (8.6%). Moreover, the fluorescence detected in the
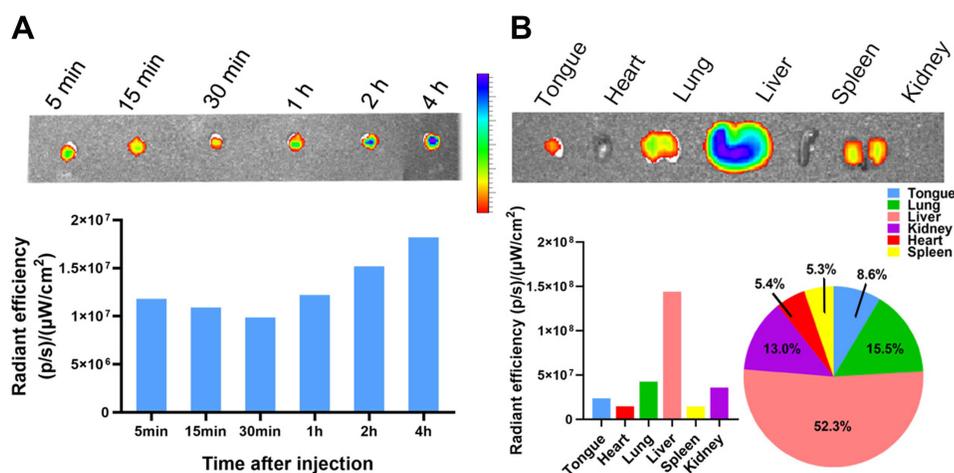

Figure 6 In vivo distribution and metabolism of DMP micelles detected by fluorescence. (**A**) DMP micelles in the mouse tongue tissue at different timepoints after i.v injection. The fluorescence intensities in tissues were detected and calculated. (**B**) Major organ distribution in mice 4 h after tail vein injection of DMP micelles with fluorescence intensities.

tongue was even higher than that in the heart and spleen, suggesting that DMP was exactly distributed systematically after intravenous injection and that the distribution in the tongue was adequate. The liver had the highest fluorescence among the main organs, which could be explained by the metabolism of DMP mostly being undertaken by the liver. Thus, based on the results of in vivo fluorescence detection, systematic administration of DMP micelles results in their accumulation in the tongue, which persists for longer than 4 h. The amount of DMP in the tongue augments with time following intravenous injection, suggesting that systematic administration might support treatment with the DMP/phBimS complex in tongue carcinoma.

We next investigated the therapeutic potential of the DMP/phBimS complex to treat the SCC15 tongue xenograft model by i.v. administration (Figure 7A). As shown in Figure 7B, as the tumor volume in the DMP/phBimS (10 μg) complex group was maintained at a stable level in our observation compared with that in the other two groups, the anti-cancer effects of DMP/phBimS were verified. At the end point of our observation, the average tongue tumor volume of the DMP/phBimS group was 16.44 mm^3, which was significantly smaller than that of the DMP/pVAX (20.36 mm^3) and NS groups (23.51 mm^3) ($P < 0.01$). Based on the tongue volume, the average inhibition rate of the DMP/phBimS group (45.63%) was higher than that of the DMP/pVAX group (12.08%) (Figure 7C). The same trend was confirmed by photographs of the tongue after euthanasia (Figure 7D and E). Mice of the DMP/phBimS group demonstrated smaller tongue volumes based on the side view and separated tongue images. Furthermore, the weights of the mice in the DMP/phBimS group were higher than those of the other two groups ($P < 0.05$), suggesting improved health of these mice (Figure S2B). We also applied H&E staining to the tongue sections to indicate the differences in volume between the three groups. The tongue sections from the DMP/phBimS group showed a smaller tumor size, while the untreated group had large tumor volumes (Figure 7F). These results suggest that the i.v. injected DMP/phBimS complex can efficiently inhibit the early growth of SCC15 tongue xenograft tumors.

We next investigated the therapeutic mechanisms. According to Figure 7G, higher Bim protein levels were detected in the DMP/phBimS group relative to the other two groups, indicating that Bim can be expressed in tumor tissue by the DMP delivery system. Regarding apoptosis-related proteins, more TUNEL-positive cells were observed in the DMP/phBimS group than in the other groups. Similar to local administration, i.v. injected DMP/phBimS led to increased expression of caspase-3 and caspase-9 protein compared with the other two groups, indicating obvious induction of apoptosis. Moreover, a higher level of CD8 was detected in the DMP/phBimS group sections, indicating enhanced infiltration of immune cells, such as monocytes and macrophages. The different expression in CD31 also indicated the anti-angiogenetic effects of the DMP/phBimS complex as the microvessel formation was decreased in DMP/phBimS group. There were no obvious pathology changes or serious adverse effects in the main organs of treated mice, indicating the safety of the DMP delivery system (Figure S3B). Additionally, there were no significant changes or toxicity in the blood circulation and some liver and kidney function indexes, with respect to MCV, MPV, HGB, MCHC, RBC, PDW, MCH, ALT, AST, γ-GT, UREA, CREA, and UA (Figure S4). These results indicate that i.v. administration of the DMP/phBimS complex facilitates anti-cancer effects by inducing apoptosis with a high degree of safety in the SCC15 mouse tongue xenograft model.

Discussion

Gene therapy has become a worthwhile supplement to current oral carcinoma treatment, including viral and non-viral based therapy.[30] Effective therapeutic targets and appropriate gene delivery vectors represent two crucial issues in oral carcinoma gene therapy studies. In the present study, we used an hBimS gene encoding plasmid delivered by a non-viral gene vector DMP cationic micelles (Scheme 1). Our results demonstrated that DMP could efficiently deliver the hBimS plasmid into cells, mainly through lipid raft-mediated and caveolin-mediated endocytosis pathways, leading to a significant anti-tumor effect of OSCC through apoptosis in vitro. The results of the mouse tongue xenograft model also indicated that our DMP/phBimS delivery system manifested significant inhibition effect of tumor proliferation through the pro-apoptosis pathway.

Gene therapy refers to treatments that introduce exogenous specific genetic material (DNA, mRNA, siRNA, or miRNA) with target roles in cells to perform functions in disease treatment and prevention.[31] Many therapy strategies have been applied in related studies, including corrective gene therapy and suicide gene therapy, to inhibit angiogenesis.
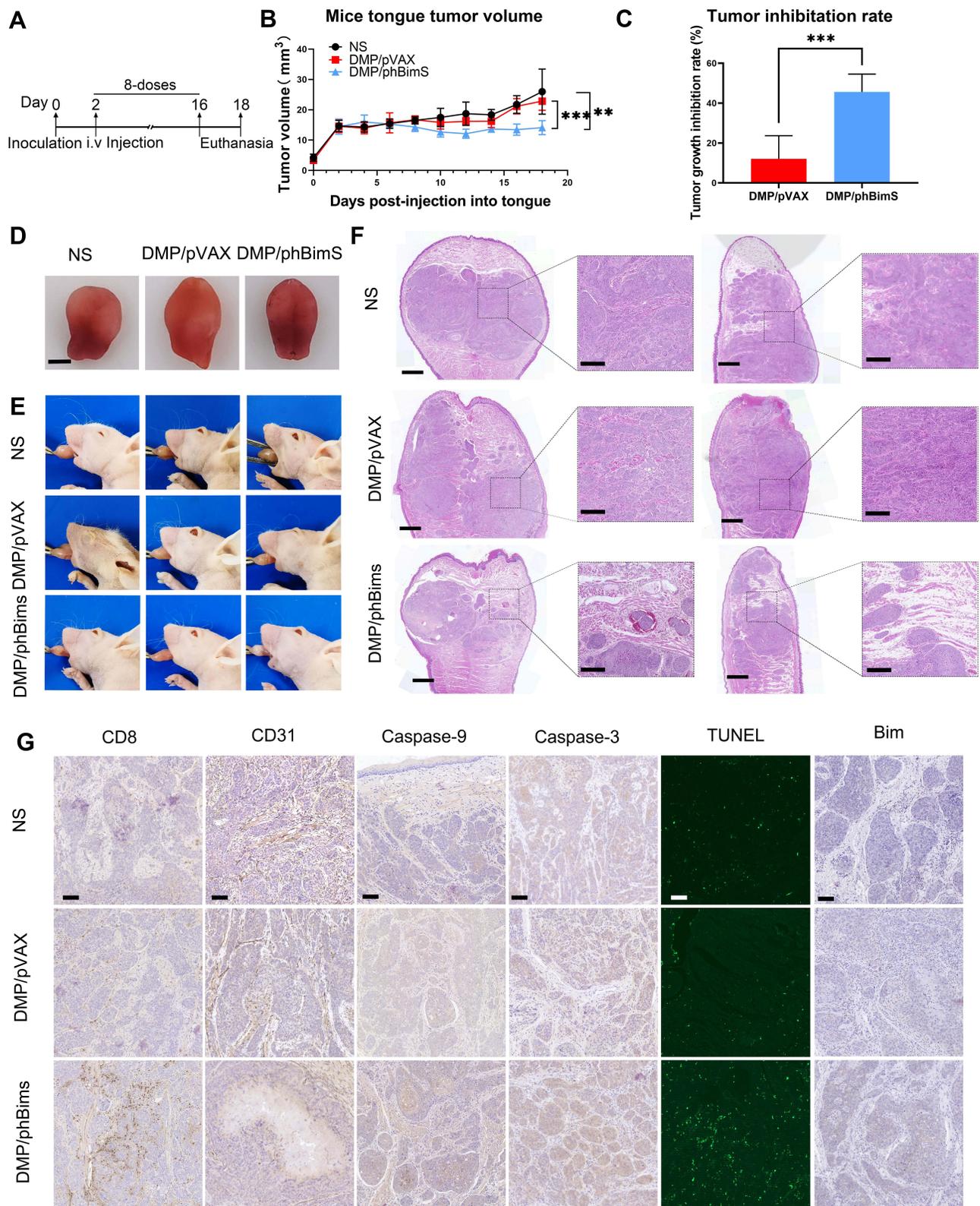
Figure 7 Therapeutic effect of the DMP/phBimS complex in tongue squamous cell tumor in vivo through systemic administration. (**A**) Schematic view of the whole experiment design and administration arrangement. (**B**) Trend of change of the mice tongue volume in each group during observation (**P < 0.01, ***P < 0.001). (**C**) Tumor growth inhibition rate in each group calculated based on tongue volume after euthanasia (***P < 0.001). (**D**) Representative isolated tongue images from each group after euthanasia (scale bar: 2.5 mm). (**E**) Representative mouse images of each group after euthanasia. (**F**) H&E analysis of tongue tissue of each group (scale bar: 750 μm for entire images; scale bar: 150 μm for partial images). (**G**) Immunohistochemical evaluation of tumor tissues from each group (scale bar: 100 μm).
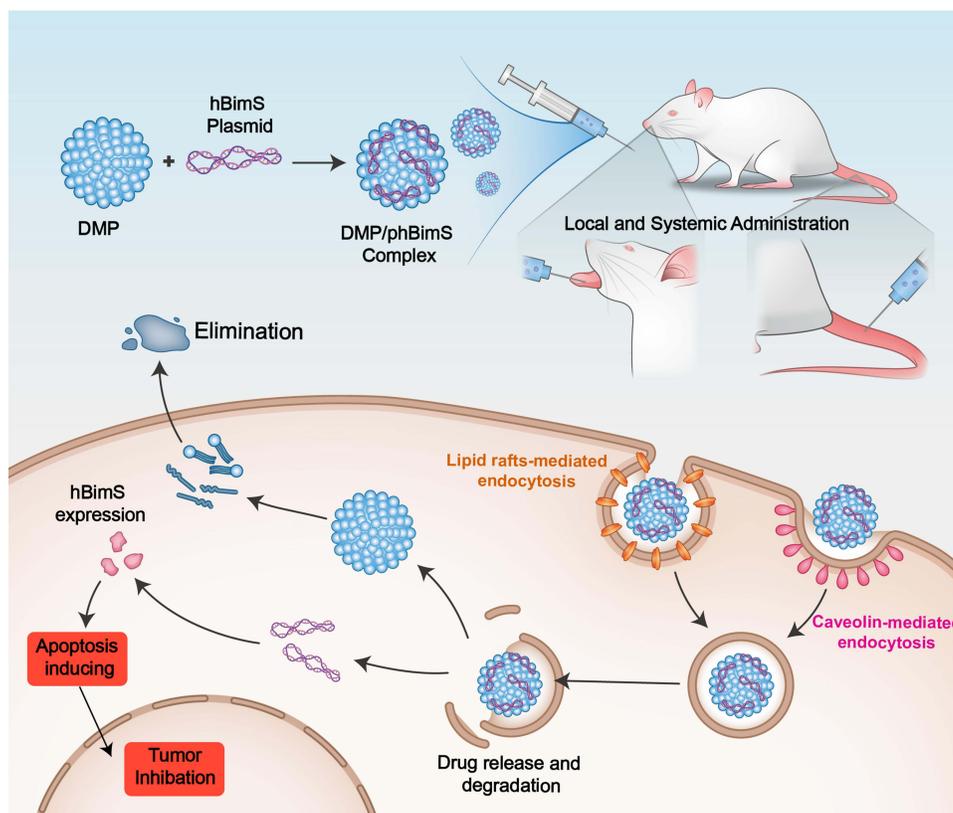
Scheme 1 An overview of the process of DMP/phBimS formulation and entry into cells to evoke tumor inhibition effects.

Suicide gene therapy is a possible choice of gene therapy in cancer, which can kill cancer cells directly or indirectly. After inducing a proapoptotic gene with appropriate viral or non-viral vectors, the viability of cancer cells is reduced, and, as cell suicide is induced under normal conditions with exogenous gene expression, nonspecific toxicity to normal tissue is reduced.[32] Thus, researchers have attempted to deliver suicide genes in studies on oral cancer gene therapy. The Herpes Simplex Virus thymidine kinase (HSV-tk)/ganciclovir (GCV) system has been used as suicide gene in related studies.[33] Neves et al used HSV-tk/GCV mediated by transferrin (Tf)-lipoplexes and confirmed the anti-tumor effect of this system in an orthotopic murine model for OSCC.[34] The results showed that this system could modify the tumor microenvironment, and lead to the recruitment of immune effector cells.[34] HSV-tk has also been used to test the effect of two plasmid vectors transfected with non-viral vector, TransfeX in oral carcinoma cells.[35] Schmidt et al[36] explored the GeneSwitch-ETA combination in FADU cells in vitro, and revealed that the use of toxin genes (pGene/V5-His-ETA) along with the GeneSwitch system can induce the treatment effect in head and neck cancer. Dias et al[37] generated a targeted oncolytic adenovirus Ad5/3-Δ24FCU1 expressing the fusion suicide gene FCU1 and verified the antitumor effect in vivo in a murine model of head and neck squamous cell carcinoma. Although the abovementioned effect was obvious, some suicide gene therapy systems consist of a suicide gene and pre-used chemotherapy drug, and some studies confirm the effect only in vitro or in a subcutaneous tumor model. Apart from the limited studies, it has been shown that effective target sites for suicide gene therapy are rare, and therefore require further investigation. In the current study, we used the DMP/phBimS delivery system in isolation, and found that this delivery system could induce significant apoptosis (33.9%) and suppression of proliferation in tongue cancer cells in vitro. Furthermore, in our mouse tongue xenograft model, this delivery system led to obvious tumor suppression, irrespective of local administration (average inhibition rate: 65.66%) or systemic administration (average inhibition rate: 45.63%). Moreover, in both route of administration, the tongue volume was smaller in the treatment group compared with the control group (7.6 mm^3 vs 22.1 mm^3, 14.1 mm^3 vs 26.0 mm^3). Compared with other studies, our research has a more completive content and used a simple non-viral vector delivery system as our DMP micelles were prepared directly by self-assembly of DOTAP with

mPEG-PCL. Thus, our findings may indicate a better perspective in future clinical treatment utility and development. Our results also indicated that the site of BimS may be an effective suicide gene target in the early growth of OSCC. Moreover, our system could work in the absence of other medicines or chemotherapy drugs, which is essential for clinical convenience. Therefore, we can conclude that our DMP/phBimS delivery system has potential use as a suicide gene therapy in early-stage OSCC.

The local administration of gene therapies usually requires lower dosages but with a limited treatment effect. OSCC is characterized by its invasion and metastasis, but local administration cannot affect its range. Moreover, local administration is often insufficient in OSCC due to the tumor location and site. Meanwhile, intravenous injection allows a high concentration of drugs to enter the blood directly after infusion, leading to more effective therapeutic action in OSCC. As a result, developing a qualified and suitable systemic administration delivery system is essential for future clinical applications. Compared with the local administration system, systemic administration requires a higher dosage; thus, the delivery system must be qualified with better biocompatible and safety, with no toxicity to other organs. For OSCC, a suitable systemic delivery system is crucial for the same reason. The systemic administration of suicide gene therapy has not yet been used in clinical situations and many experts have attempted to use their drug systems in animal models of different cancers. For example, the polyplex micelle system (PM) vectors have been used by Tockary et al with a combination of single-stranded DNA (ssDNA) systemically administered in a pancreatic cancer mouse model, in which an antitumor effect was noted.[38] Similarly, Gao et al[39] also used the non-viral vector PEI-PLL-PEG-angiopep-2 (PPA)/DNA nanoparticles (NPs) in glioma-targeting treatment and demonstrated that the vector could cross the blood brain barrier. By combined with HSV-tk, the polymer/HSV-tk NPs showed anti-glioma effects and a significant survival benefit in an orthotopic human GBM mouse model via intravenous (i.v.) injection. Meanwhile other experts have explored the systemic use of viral vectors. Han et al attempted to use adenovirus as vectors treating liver cancer through systemic administration and demonstrated an efficient anticancer effect and minimal liver toxicity.[40] Generally, vectors must be adopted to realize systematic administration delivery, but only a few vectors satisfy the requirements of safety and delivery efficiency, and have metabolic and distribution characteristics in suicide gene therapy. However, until now, studies in OSCC have been limited and qualified viral or non-viral vectors are not abundant for suicide gene therapy. In this study, we prepared a single vector named DMP. As DMP has been used for systemic administration in animal models several times,[25,41] we attempted to use it as a delivery vector for OSCC suicide gene therapy. We evaluated the protection quality, safety, distribution, and metabolism in mouse models of DMP. As result, we found no obvious toxicity in the main organs of mice following systemic administration of the DMP/phBimS complex. The complex could also distribute a sufficient dosage to the tongue area after systemic administration according to fluorescence imaging, with the highest fluorescence detected in the liver (52.3%), indicating that most metabolic processes of DMP occurred in the liver. These results indicated that DMP is capable of systemic administration in mice, with acceptable distribution and metabolism and no toxicity to the main organs. These characteristics make it suitable for further research as a potential gene therapy system. Furthermore, DMP can be detected in the tongue for an extended duration after intravenous injection, which is also the basis of systemic administration. We successfully used the DMP/phBimS system to realize the intravenous injection of systemic administration in the SCC15 mouse tongue xenograft model. The antitumor effect was obvious, together with suitable safety and biodegradation, and no damage to the major organs of mice after successive drug injection. The possible reasons for this achievement include the high delivery efficiency of our cationic nanoparticle micelles DMP. The results showed that the delivery efficiency was $52.07\% \pm 1.63\%$ for SCC15 cells in vitro and the hBimS plasmid could express corresponding protein following delivery into cells. Moreover, this delivery system could distribute to the tongue area and remain for at least 4 h. Gathering of the drug in the tongue area ensures its pro-apoptosis effect. Furthermore, our DMP/phBimS system displayed sufficient biocompatibility and safety, as there was no obvious damage observed in the major organs. Therefore, we successfully used the DMP/phBimS suicide gene therapy delivery system to obtain an anti-tumor effect through apoptotic pathway in early-stage OSCC by systemic administration, with demonstrable safety.

Conclusion

In conclusion, we synthesized self-assembled DMP cationic micelles using the block polymer MPEG–PCL and cationic lipid DOTAP. Combined with a plasmid encoding human BimS protein, we demonstrated the DMP could deliver hBimS plasmid into SCC15 in vitro and express hBimS protein, which led to a significant inhibition effect on cell proliferation through the apoptosis pathway. In addition, we demonstrated that the DMP could remain in the tongue for an extended

duration after intravenous injection, with adequate safety for systemic administration. Moreover, both local and systemic administration in the mouse tongue xenograft model could represent a significant antitumor effect in early-stage tumor growth. The DMP/phBimS non-viral suicide gene therapy system has the potential utility for oral squamous carcinoma treatment in the future.

Acknowledgments

Disclosure

The authors report no conflicts of interest in this work.

References

1. Warnakulasuriya S. Global epidemiology of oral and oropharyngeal cancer. *Oral Oncol*. 2009;45(4–5):309–316. doi:10.1016/j. oraloncology.2008.06.002
2. Bray F, Ferlay J, Soerjomataram I, Siegel RL, Torre LA, Jemal A. Global cancer statistics 2018: GLOBOCAN estimates of incidence and mortality worldwide for 36 cancers in 185 countries. *CA Cancer J Clin*. 2018;68(6):394–424. doi:10.3322/caac.21492
3. Zhao J, Liu D, Yang H, Yu S, He H. Long noncoding RNAs in head and neck squamous cell carcinoma: biological functions and mechanisms. *Mol Biol Rep*. 2020;47(10):8075–8090. doi:10.1007/s11033-020-05777-w
4. Huang SH, O'Sullivan B. Oral cancer: current role of radiotherapy and chemotherapy. *Med Oral Patol Oral Cir Bucal*. 2013;18(2):e233–240. doi:10.4317/medoral.18772
5. Birkeland AC, Ludwig ML, Spector ME, Brenner JC. The potential for tumor suppressor gene therapy in head and neck cancer. *Discov Med*. 2016;21(113):41–47.
6. Peng Z. Current status of gendicine in China: recombinant human Ad-p53 agent for treatment of cancers. *Hum Gene Ther*. 2005;16(9):1016–1027. doi:10.1089/hum.2005.16.1016
7. Lonez C, Vandenbranden M, Ruysschaert JM. Cationic liposomal lipids: from gene carriers to cell signaling. *Prog Lipid Res*. 2008;47(5):340–347. doi:10.1016/j.plipres.2008.03.002
8. Liang Q, Monetti C, Shutova MV, et al. Linking a cell-division gene and a suicide gene to define and improve cell therapy safety. *Nature*. 2018;563 (7733):701–704. doi:10.1038/s41586-018-0733-7
9. Pinsky MS, Song W, Dong Z, et al. Activation of iCaspase-9 in neovessels inhibits oral tumor progression. *J Dent Res*. 2006;85(5):436–441. doi:10.1177/154405910608500508
10. Li Y, Li B, Li CJ, Li LJ. Key points of basic theories and clinical practice in rAd-p53 (Gendicine ™) gene therapy for solid malignant tumors. *Expert Opin Biol Ther*. 2015;15(3):437–454. doi:10.1517/14712598.2015.990882
11. Tang W, He Y, Zhou S, Ma Y, Liu G. A novel Bifidobacterium infantis-mediated TK/GCV suicide gene therapy system exhibits antitumor activity in a rat model of bladder cancer. *J Exp Clin Cancer Res*. 2009;28(1):155. doi:10.1186/1756-9966-28-155
12. Chi X, Nguyen D, Pemberton JM, et al. The carboxyl-terminal sequence of bim enables bax activation and killing of unprimed cells. *Elife*. 2020;9: e44525. doi:10.7554/eLife.44525
13. Yamaguchi T, Okada T, Takeuchi K, et al. Enhancement of thymidine kinase-mediated killing of malignant glioma by BimS, a BH3-only cell death activator. *Gene Ther*. 2003;10(5):375–385. doi:10.1038/sj.gt.3301897
14. Giam M, Huang DC, Bouillet P. BH3-only proteins and their roles in programmed cell death. *Oncogene*. 2008;27(Suppl 1):S128–136. doi:10.1038/ onc.2009.50
15. Baumgartner U, Berger F, Hashemi Gheinani A, Burgener SS, Monastyrskaya K, Vassella E. miR-19b enhances proliferation and apoptosis resistance via the EGFR signaling pathway by targeting PP2A and BIM in non-small cell lung cancer. *Mol Cancer*. 2018;17(1):44. doi:10.1186/ s12943-018-0781-5
16. Wu D, Chen B, Cui F, He X, Wang W, Wang M. Hypoxia-induced microRNA-301b regulates apoptosis by targeting Bim in lung cancer. *Cell Prolif*. 2016;49(4):476–483. doi:10.1111/cpr.12264
17. Merino D, Best SA, Asselin-Labat ML, et al. Pro-apoptotic Bim suppresses breast tumor cell metastasis and is a target gene of SNAI2. *Oncogene*. 2015;34(30):3926–3934. doi:10.1038/onc.2014.313
18. Yin H, Kanasty RL, Eltoukhy AA, Vegas AJ, Dorkin JR, Anderson DG. Non-viral vectors for gene-based therapy. *Nat Rev Genet*. 2014;15 (8):541–555. doi:10.1038/nrg3763
19. Saxena V, Hussain MD. Polymeric mixed micelles for delivery of curcumin to multidrug resistant ovarian cancer. *J Biomed Nanotechnol*. 2013;9 (7):1146–1154. doi:10.1166/jbn.2013.1632
20. Prabhu P, Patravale V. The upcoming field of theranostic nanomedicine: an overview. *J Biomed Nanotechnol*. 2012;8(6):859–882. doi:10.1166/ jbn.2012.1459
21. Palazzolo S, Bayda S, Hadla M, et al. The clinical translation of organic nanomaterials for cancer therapy: a focus on polymeric nanoparticles, micelles, liposomes and exosomes. *Curr Med Chem*. 2018;25(34):4224–4268. doi:10.2174/0929867324666170830113755
22. Sun L, Wu Q, Peng F, Liu L, Gong C. Strategies of polymeric nanoparticles for enhanced internalization in cancer therapy. *Colloids Surf B Biointerfaces*. 2015;135:56–72. doi:10.1016/j.colsurfb.2015.07.013

23. Blasco MA, Svider PF, Raza SN, et al. Systemic therapy for head and neck squamous cell carcinoma: historical perspectives and recent breakthroughs. *Laryngoscope*. 2017;127(11):2565–2569. doi:10.1002/lary.26629

24. Rahman MA, Amin AR, Wang X, et al. Systemic delivery of siRNA nanoparticles targeting RRM2 suppresses head and neck tumor growth. *J Control Release*. 2012;159(3):384–392. doi:10.1016/j.jconrel.2012.01.045

25. Duan X, Wang P, Men K, et al. Treating colon cancer with a suicide gene delivered by self-assembled cationic MPEG-PCL micelles. *Nanoscale*. 2012;4(7):2400–2407. doi:10.1039/c2nr30079f

26. Men K, Huang R, Zhang X, et al. Local and systemic delivery of interleukin-12 gene by cationic micelles for cancer immunogene therapy. *J Biomed Nanotechnol*. 2018;14(10):1719–1730. doi:10.1166/jbn.2018.2593

27. Men K, Liu W, Li L, et al. Delivering instilled hydrophobic drug to the bladder by a cationic nanoparticle and thermo-sensitive hydrogel composite system. *Nanoscale*. 2012;4(20):6425–6433. doi:10.1039/c2nr31592k

28. Suzuki S, Toyoma S, Tsuji T, Kawasaki Y, Yamada T. CD147 mediates transforming growth factor-β1-induced epithelial-mesenchymal transition and cell invasion in squamous cell carcinoma of the tongue. *Exp Ther Med*. 2019;17(4):2855–2860. doi:10.3892/etm.2019.7230

29. Rahi D, Dzyuba B, Xin M, Cheng Y, Dzyuba V. Energy pathways associated with sustained spermatozoon motility in the endangered Siberian sturgeon Acipenser baerii. *J Fish Biol*. 2020;97(2):435–443. doi:10.1111/jfb.14382

30. Kojima Y, Otsuki N, Kubo M, et al. Adenovirus-mediated transfer of HPV 16 E6/E7 antisense RNA combined with cisplatin inhibits cellular growth and induces apoptosis in HPV-positive head and neck cancer cells. *Cancer Gene Ther*. 2018;25(9–10):274–283. doi:10.1038/s41417-018-0024-3

31. Gebremedhin S, Singh A, Koons S, Bernt W, Konopka K, Duzgunes N. Gene delivery to carcinoma cells via novel non-viral vectors: nanoparticle tracking analysis and suicide gene therapy. *Eur J Pharm Sci*. 2014;60:72–79. doi:10.1016/j.ejps.2014.03.003

32. Di Stasi A, Tey SK, Dotti G, et al. Inducible apoptosis as a safety switch for adoptive cell therapy. *N Engl J Med*. 2011;365(18):1673–1683. doi:10.1056/NEJMoa1106152

33. Yu D, Wang A, Huang H, Chen Y. PEG-PBLG nanoparticle-mediated HSV-TK/GCV gene therapy for oral squamous cell carcinoma. *Nanomedicine*. 2008;3(6):813–821. doi:10.2217/17435889.3.6.813

34. Neves S, Faneca H, Bertin S, et al. Transferrin lipoplex-mediated suicide gene therapy of oral squamous cell carcinoma in an immunocompetent murine model and mechanisms involved in the antitumoral response. *Cancer Gene Ther*. 2009;16(1):91–101. doi:10.1038/cgt.2008.60

35. Düzgüneş N, Cheung J, Konopka K. Non-viral suicide gene therapy in cervical, oral and pharyngeal carcinoma cells with CMV- and EEV-plasmids. *J Gene Med*. 2018;20(10–11):e3054. doi:10.1002/jgm.3054

36. Schmidt M, Gruensfelder P, Roller J, Hagen R. Suicide gene therapy in head and neck carcinoma cells: an in vitro study. *Int J Mol Med*. 2011;27(4):591–597. doi:10.3892/ijmm.2011.610

37. Dias JD, Liikanen I, Guse K, et al. Targeted chemotherapy for head and neck cancer with a chimeric oncolytic adenovirus coding for bifunctional suicide protein FCU1. *Clin Cancer Res*. 2010;16(9):2540–2549. doi:10.1158/1078-0432.ccr-09-2974

38. Tockary TA, Foo W, Dirisala A, et al. Single-stranded DNA-packaged polyplex micelle as adeno-associated-virus-inspired compact vector to systemically target stroma-rich pancreatic cancer. *ACS Nano*. 2019;13(11):12732–12742. doi:10.1021/acsnano.9b04676

39. Gao S, Tian H, Xing Z, et al. A non-viral suicide gene delivery system traversing the blood brain barrier for non-invasive glioma targeting treatment. *J Control Release*. 2016;243:357–369. doi:10.1016/j.jconrel.2016.10.027

40. Han SR, Lee CH, Im JY, et al. Targeted suicide gene therapy for liver cancer based on ribozyme-mediated RNA replacement through post-transcriptional regulation. *Mol Ther Nucleic Acids*. 2021;23:154–168. doi:10.1016/j.omtn.2020.10.036

41. Li J, Men K, Gao Y, et al. Single micelle vectors based on lipid/block copolymer compositions as mRNA formulations for efficient cancer immunogene therapy. *Mol Pharm*. 2021;18(11):4029–4045. doi:10.1021/acs.molpharmaceut.1c00461